

# PCCP

Accepted Manuscript



This is an *Accepted Manuscript*, which has been through the Royal Society of Chemistry peer review process and has been accepted for publication.

*Accepted Manuscripts* are published online shortly after acceptance, before technical editing, formatting and proof reading. Using this free service, authors can make their results available to the community, in citable form, before we publish the edited article. We will replace this *Accepted Manuscript* with the edited and formatted *Advance Article* as soon as it is available.

You can find more information about *Accepted Manuscripts* in the [Information for Authors](#).

Please note that technical editing may introduce minor changes to the text and/or graphics, which may alter content. The journal's standard [Terms & Conditions](#) and the [Ethical guidelines](#) still apply. In no event shall the Royal Society of Chemistry be held responsible for any errors or omissions in this *Accepted Manuscript* or any consequences arising from the use of any information it contains.

# Theoretical study of small sodium-potassium alloy clusters through genetic algorithm and quantum chemical calculations<sup>†</sup>

Mateus X. Silva, Breno R. L. Galvão and Jadson C. Belchior

Received Xth XXXXXXXXXXXX 20XX, Accepted Xth XXXXXXXXXXXX 20XX

First published on the web Xth XXXXXXXXXXXX 200X

DOI: 10.1039/b000000x

Genetic algorithm is employed to survey an empirical potential energy surface for small  $\text{Na}_x\text{K}_y$  clusters with  $x+y \leq 15$ , providing initial conditions for electronic structure methods. The minima of such empirical potential are assessed and corrected using high level *ab initio* methods such as CCSD(T), CR-CCSD(T)-L and MP2, and benchmark results are obtained for specific cases. The results are the first calculations for such small alloy clusters and may serve as a reference for further studies. The validity and choice of a proper functional and basis set for DFT calculations are then explored using the benchmark data, where it was found that the usual DFT approach may fail to provide the correct qualitative result for specific systems. The best general agreement to the benchmark calculations is achieved with def2-TZVPP basis set with SVWN5 functional, although the LANL2DZ basis set (with effective core potential) and SVWN5 functional provided the most cost-effective results.

## 1 Introduction

Metal clusters have attracted a large scientific effort due to their potential as technological applications at the nano-scale. The theoretical concerns go beyond the structure of such systems, and a major aim is the understanding of how they grow and how properties change in the course of this process. The NaK alloy is known to be miscible in all proportions and is liquid at room temperature for most compositions<sup>1</sup>. Such cluster has found theoretical and experimental discussion specially for large numbers of atoms<sup>1–6</sup>, where it was shown that potassium atoms tend to agglomerate on the surface. However, within the growth and structural analysis, little attention has been given to this alloy, on the contrary of what happens to its pure counterparts.

In this work we are interested in the description of the NaK clusters starting from small amounts of atoms, where we can assess the validity of electronic structure methods and empirical potentials available for generating the electronic potential energy surface. Therefore we tackle the problem by first using a Gupta<sup>7,8</sup> type analytic potential, coupled to efficient optimization by genetic algorithms (GAs), followed by verifying their validity using the best affordable electronic structure method.

Given that the theoretical effort necessary to calculate the electronic potential energy increases largely with the number

of atoms and electrons in the system, high level calculations are generally not affordable even for a single point energy, not to mention the immense task of optimizing the  $3N - 6$  degrees of freedom of a  $N$ -atom system. Thus, an effective density functional theory (DFT) treatment of the system would be desirable in order to allow the calculations for larger clusters within a quantum chemical approach. In this view, one of the main focuses here is to obtain a set of functional and basis set for DFT calculations for the NaK alloy, capable of reproducing benchmark high level *ab initio* calculations performed here for the alloys and to other data available in the literature for pure Na and K clusters (since previous work on alkali binary clusters is rather scarce<sup>5</sup>).

The paper is divided as follows: Section 2.1 gives a brief description of the Gupta analytic potential, while Section 2.2 exposes the GA method. The details of the electronic structure calculations are given in Section 2.3 and the results are discussed in Section 3. Section 4 gathers the main conclusions.

## 2 Methodology

### 2.1 Empirical potential

For the search of global minima with the GA approach, the Gupta potential function<sup>7,8</sup> was employed for a fast evaluation of the potential energy (GA/Gupta). Based on the second moment approximation to tight-binding theory, this potential is largely used and has been optimized for alkali metal clusters by Li *et al.*<sup>9</sup>. Within this approach, the total energy of an  $N$ -atom cluster ( $V_{clus}(N)$ ) is written as a sum over atomic con-

<sup>†</sup> Electronic Supplementary Information (ESI) available. See DOI: 10.1039/b000000x/

Departamento de Química-ICEx, Universidade Federal de Minas Gerais, Av. Antônio Carlos 6627, Pampulha, (31.270-901) Belo Horizonte, Minas Gerais, Brazil

E-mail: jadson@ufmg.br

tributions  $E_i$ , which are decomposed into an attractive band-energy many-body term and a repulsive pairwise contribution as  $E_i = E_i^{\text{band}} + E_i^{\text{rep}}$ . Each term is given by

$$E_i^{\text{band}} = - \left\{ \sum_{j \neq i}^N \xi^2 \exp \left[ -2q \left( \frac{r_{ij}}{r_0} - 1 \right) \right] \right\}^{1/2} \quad (1)$$

$$E_i^{\text{rep}} = \sum_{j \neq i}^N A \exp \left[ -p \left( \frac{r_{ij}}{r_0} - 1 \right) \right] \quad (2)$$

where  $r_{ij}$  is the distance between atoms  $i$  and  $j$ . The parameters  $q$ ,  $p$ ,  $\xi$  and  $A$  were fitted<sup>9</sup> to local density approximation database for sodium and potassium,  $r_0$  is a scaling factor for the distances between atoms, usually identified with the nearest-neighbor distance in the bulk metal. For the heteronuclear bonds of NaK, we have followed Ref. 5 and used the average over the parameters for Na and K determined by Li *et al.*<sup>9</sup>.

## 2.2 Genetic algorithm

In the search for the minima available in the potential energy hypersurface, we have employed the standard genetic algorithm improved by two new operators<sup>10</sup>. Briefly, for a given system the Cartesian coordinates are generated randomly multiple times for each atom, providing a population of molecular configurations, which is used by the GA to build a unique gene (as given in Ref. 11). In our approach, we take the extra step of relaxing each cluster of the population to its closest local minimum using the quasi-Newtonian BFGS method<sup>12</sup>, followed by evolving one generation by applying the standard set of genetic operators (cross-over, mutation and natural selection). This avoids moving too soon from a certain region of the PES to another without “exploring” such region. The parents for crossover are selected with some variant of the roulette-wheel method<sup>13</sup> and the fitness function determined for each cluster of the population, according to<sup>14</sup>:

$$F_i = \frac{1}{2} \left[ 1 - \tanh \left( 2 \frac{E_i - E_{\min}}{E_{\max} - E_{\min}} - 1 \right) \right] \quad (3)$$

where  $E_{\max}$  and  $E_{\min}$  are the maximum and minimum potential energies for the current population. For mating between two parents (cross-over) one cut them about a randomly oriented plane, exchanging the complementary fragments and splicing them together to form two new offspring<sup>11,13</sup>. The next operation (mutation) consists of changing the originated subpopulation of offspring, where a constant probability for mutation (15%) has been assigned to each one. Mutation is incorporated by rotating parts of each cluster by random amounts. At this stage, our approach<sup>10</sup> differs from the standard GA by adding the annihilator operator, which removes offspring and mutants with the same energies as preexisting members of the population. The history operator keeps a record of the initial population for future use. One then selects the  $N_{\text{pop}}$  clusters

with lowest energy from a ranked list in order of potential energy and discards the rest. The above mentioned procedures constitute one step for the GA, which are repeated for a specific number of generations until convergence. For a standard GA this would mean that the lowest possible minimum has been found within the method, but it may happen that a non-optimal solution has been found (there exists a deeper minimum). In order to check this, new cycles of generations are performed but with the initial population provided by the history operator (instead of randomly). The history operator is applied only after a mass extinction is promoted by the annihilator operator, that is, deleting all structures. This procedure is only halted if after a predetermined number of cycles a structure with lower energy than the current minimum is not found, and has been shown to yield improved results for systems of water clusters and metallic nanoalloys of gold and copper<sup>10,14</sup>.

## 2.3 Electronic structure

All electronic structure calculations were performed using the GAMESS<sup>15</sup> package. In a first instance, the structures provided by the Gupta empirical potential were re-optimized using 6-311+G\* and def2-TZVPP basis set with Møller-Plesset second order perturbation theory (MP2) including (3s, 3p) correlation for K and keeping only the inner core (1s) electrons frozen for Na. As a next step, the aug-cc-pVTZ (or simply VTZ) basis sets belonging to the correlation-consistent family<sup>16,17</sup> were tested for sodium. Since the latter is not available for potassium, different basis were tested, namely the def2-SVP and def2-TZVPP<sup>18</sup> from the basis set exchange library<sup>19</sup>.

For the smallest closed and open shell systems, we have performed coupled-cluster singles and doubles with perturbative triples (CCSD(T)<sup>20</sup>) and completely renormalized coupled-cluster (CR-CCSD(T)-L) calculations respectively, for both optimizing the geometry and obtaining the frequencies of the stationary points.

For the DFT approach, B3LYP<sup>21–23</sup>, PW91<sup>24</sup>, PBE<sup>25</sup> and SVWN5<sup>26,27</sup> exchange and correlation functionals were tested with different basis sets. The inclusion of subvalence correlation turns out to be important for K and strongly recommended for Na as demonstrated in Ref. 28, and thus DFT calculations were also performed with the LANL2DZ basis set with an effective core potential (ECP). The results were compared to all-electrons coupled-cluster ones for smaller systems.

For all the approaches discussed in this section, a restricted Hartree-Fock (RHF) self-consistent field wavefunction was employed in the calculations concerning closed shell systems, while restricted open shell Hartree-Fock (ROHF) was adopted for spin multiplicities other than one, in order to avoid spin contamination.

### 3 Results

#### 3.1 GA structures

The standard GA approach (and also the basin hopping method) has been employed by Lai *et al.*<sup>29</sup> for homogeneous clusters of Na, K, Rb, and Cs using the Gupta potential, and before starting the  $\text{Na}_x\text{K}_y$  alloy calculations, we have also used our GA approach for the  $\text{Na}_n$  and  $\text{K}_n$  for  $2 < n < 15$  to compare with the former results. Apart from small deviations, such as more compact structures, the geometrical shapes are essentially the same, indicating, in principle, that the ones calculated in Ref. 29 were already the global minima.

When studying the growth of clusters, it is helpful to compare the energy of a structure with  $N$  atoms, against the neighbors  $N - 1$  and  $N + 1$  to explore the relative stability. This is calculated by the second energy difference, which can be helpful on the prediction of possible magic numbers of atoms in clusters<sup>30</sup>, and its expression is given below:

$$\Delta_2 E_b(N) = 2E_b(N) - E_b(N - 1) - E_b(N + 1) \quad (4)$$

where  $E_b$  is the average bond energy, given by  $E_b = -V_{clus}/N$ . In Fig. 1 the second energy difference both for sodium and potassium are presented, where a similar pattern is clear. The peaks that can be seen at 4, 6 and 13 atoms indicate a relative stability of them against the neighbouring numbers of atoms composing the clusters. These peaks correspond, as expected, to the most symmetric geometries found among all the number of atoms studied here, which are respectively a tetrahedron, an octahedron and an icosahedron. The clusters of 13 atoms are of special importance since it is the smallest possible Mackay icosahedron for the growth of the cluster, and therefore may be more amenable for higher levels of calculations. Also seen in this graph is that the sodium clusters have second energy differences slightly higher than those of potassium. For a more in depth discussion of such homonuclear clusters, the reader is addressed to Ref. 29.

The main focus of this work is on sodium potassium alloys. This is a much harder task than to describe the homonuclear counterpart, given that for each nuclearity several compositions are possible, and the cartesian coordinates of the global minima found here for all compositions with  $x + y \leq 15$  are given as supplementary material. For one example, we consider the growth by adding sodium atoms one by one on a single potassium atom, and also the reciprocal (adding potassium on a sodium atom), which will prove helpful to elucidate general properties of the growth. The structures obtained for  $\text{Na}_x\text{K}_1$  are shown in Fig. 2, where all structures resemble the geometry of pure Na clusters, except for the elongated bond lengths observed around the potassium atom. A noteworthy aspect about these alloys is the general tendency observed of the K atoms to stay on the surface for all the compositions

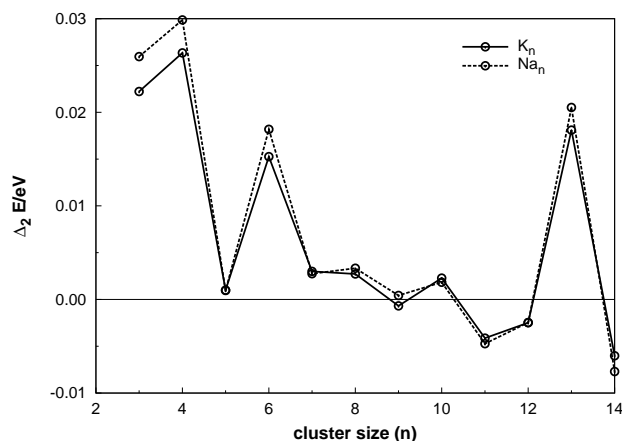


**Fig. 1** Second energy difference for the sodium and potassium homonuclear clusters.

tested, as previously found for 55 atom NaK clusters except at the dilute concentration limits of sodium<sup>5</sup> and expected also on the experimental side, where evidence for such behavior was found by using synchrotron-based photoelectron spectroscopy<sup>1</sup>.

In a first approximation, it can be argued that for an alloy cluster  $\text{A}_x\text{B}_y$  with the A-B bond strength stronger than A-A or B-B, mixing will be favored, while segregation will manifest in the other cases. Since we have fixed the Gupta parameters that will control the strength for the Na-K bond as averages, it cannot be stronger than both Na-Na and K-K, and segregation is expected, as shown in Fig. 2. Only the electronic structure calculations can remove this bias and corroborate or not to the Gupta/GA results.

An interesting feature is that at clusters size of 10 we can already see the development of an icosahedron, just lacking some corners, which atom after atom starts completing until the final shape at  $N = 13$ . The addition of an extra sodium does not change the former icosahedral shape, but after the addition of a second atom a new polygon is formed.

Although the structures of the  $\text{Na}_x\text{K}_1$  are notably similar to the homonuclear counterparts, the picture is changed for the  $\text{Na}_1\text{K}_y$  case (Fig. 3) where for the cluster of sizes  $N = 9$  and 10 a change in shape is observed: there is a central atom. This is due to the tendency of sodium to occupy the center and K be segregated at the surface, which has been observed experimentally<sup>1</sup>.

The second energy differences for the alloy growing with one atom fixed is given in Fig. 4, where it is seen that the  $\text{Na}_x\text{K}_1$  is closely related to that of the homonuclear clusters. The  $\text{Na}_1\text{K}_y$  has also a similar shape, except for the differences in the vicinity of  $N = 9$  and 10 which shows different structures, as discussed above.

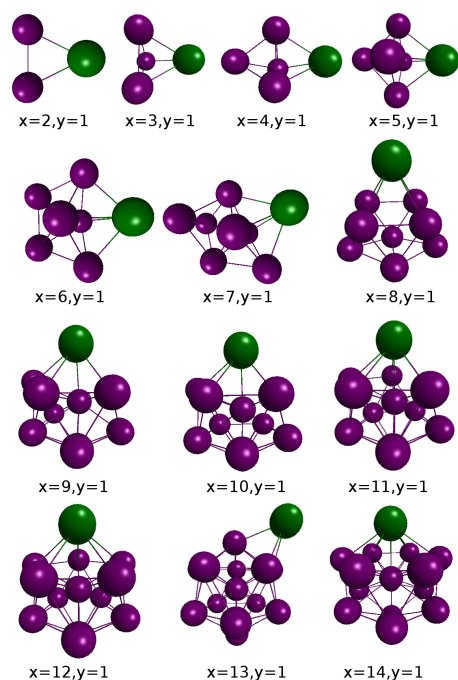


**Fig. 2** Structures of the  $\text{Na}_x\text{K}_y$  clusters for the growth by adding Na (purple) atoms on a single K (green), optimized in the GA/GUPTA approach.

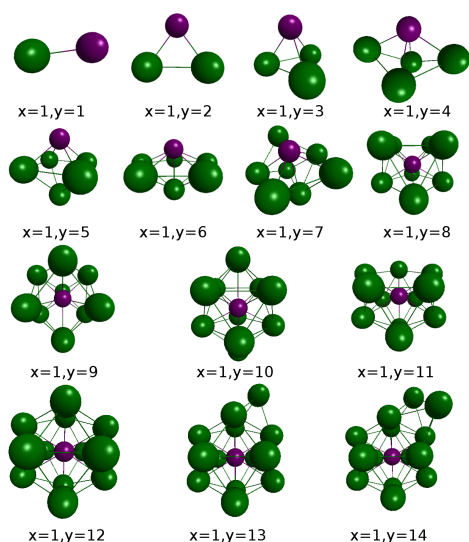


**Fig. 3** Structures of the  $\text{Na}_x\text{K}_y$  clusters for the growth by adding K (green) atoms on a single Na (purple), optimized in the GA/GUPTA approach.

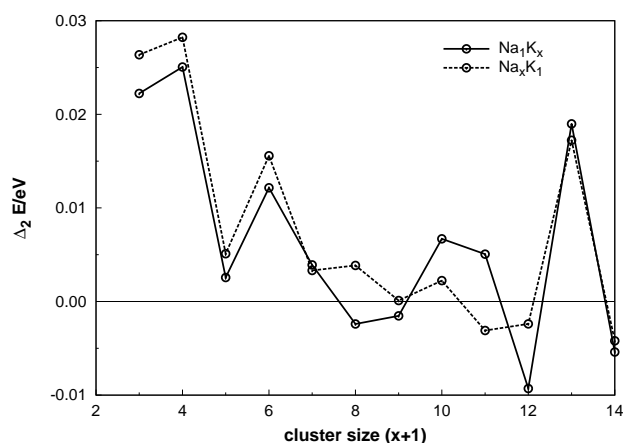


**Fig. 4** Second energy difference for the clusters with a single dopant atom.

The tetrahedron structure found by the Gupta potential for the homonuclear clusters of four atoms is in conflict with the available literature data<sup>31–33</sup> that indicates a planar configuration. For this reason we turn now to the reliability of the empirical potential approach for small sized clusters by performing *ab initio* calculations.

### 3.2 *Ab initio* results

Even assuming that the GA approach has found the best structures possible, the Gupta potential may not be suitable to be used outside its range of applicability. For example, the parameters used for the Na-Na and K-K interactions were fitted by Li *et al.*<sup>9</sup> to a local density approximation database. The latter consists of the total energy as a function of the lattice constant, and therefore structures found by the GA method for small clusters may be out of the scope of the potential. In fact, there is experimental evidence<sup>31</sup> stating that the potassium trimer ( $\text{K}_3$ ) has  $C_{2v}$  symmetry and  $\text{K}_4$  has a planar diamond shape ( $D_{2h}$ ), whereas the Gupta results predict more symmetrical structures ( $D_{3h}$  and  $T_d$ , respectively).

Since we want to assess the validity of the structures obtained in the previous section, we perform accurate benchmark calculations for the smallest clusters and study the validity of different quantum approaches for clusters with less than ten atoms. This will also be useful to predict what type of electronic structure calculation will be most suitable for larger clusters. The benchmark results correspond to all-electrons correlated coupled cluster calculations with the def2-TZVPP basis set, and are given in Table 1 for the three and four atoms clusters. The results agree with the available literature data for the pure clusters, with all 4 atom alloys showing planar diamond shapes. The two triatomic alloys show bent structures,

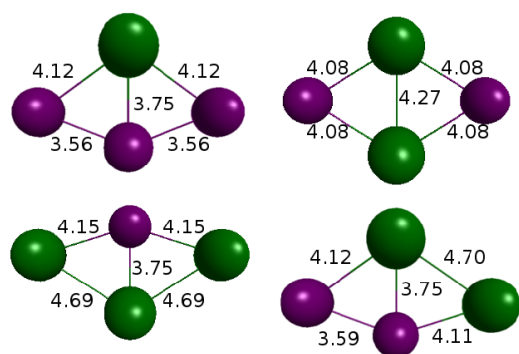


**Fig. 5** Frozen core CCSD(T) calculations for the four atom sodium (purple)/potassium (green) clusters. Bond lengths are given in Å.

and the  $\text{Na}_2\text{K}_1$  is even slightly asymmetric, with one bond length differing by  $0.03\text{Å}$  from the other. There is also a linear isomer for this species, but our calculations show that the bent one is the global minimum. To the best of our knowledge, the present geometries predicted at these levels of calculation for the alloys have not been reported before.

We have also explored the quartet states of  $\text{Na}_3$  and  $\text{K}_3$  which turned out to have minima as equilateral triangles, as predicted previously by the Gupta potential in this work with the GA methodology. However, in contrast to the empirical potential, the bond distances are too large indicating van der Waals structures as analysed in Ref. 35.

It is known that the correlation of the core electrons plays an important role for heavier atoms such as potassium, and it would be desirable to test whether this effect is necessary to reproduce the shape of the clusters. In case a satisfactory description could be obtained without including this extremely time consuming feature, we could employ such methodology for larger clusters. For the four atom alloys, the benchmark calculation in Table 1 can be compared to the frozen-core coupled cluster ones of Fig. 5. The latter results are not only in qualitative agreement (planar and diamond-shaped), but also the bond lengths seem to be well represented. The comparison also corroborates previous predictions<sup>31,36</sup> that core electron polarization causes additional contraction of the bonds lengths. Two different isomers were found and are shown in Fig. 5 for  $\text{Na}_2\text{K}_2$ , but the more symmetrical one has lower energy.

The widely used Dunning's basis sets (cc-pVXZ) are not available for the potassium atom. In order to compare it with the def2-TZVPP<sup>18</sup> one, we have optimized the  $\text{Na}_4$  cluster with both of them, and also compared the results with the all-electron treatment with the def2-TZVPP basis, being the results presented in Table 2. Although the latter basis set is not specifically fitted to the actual case, it showed a perfect agree-

**Table 1** All-electrons CR-CCSD(T)-L and CCSD(T) calculations for 3 and 4 atoms clusters respectively, employing the def2-TZVPP basis set. Distances in Å and angles in degrees.

system	property	benchmark
$\text{Na}_3$	$R_{12}$	3.25
	$R_{13}$	3.25
	$\theta$	79.15
$\text{Na}_2\text{K}_1$	$R_{\text{KNa}_A}$	3.70
	$R_{\text{KNa}_B}$	3.70
	$\theta$	62.69
$\text{Na}_1\text{K}_2$	$R_{\text{NaK}_A}$	3.72
	$R_{\text{NaK}_B}$	3.69
	$\theta$	100.69
$\text{K}_3^a$	$R_{12}$	4.10
	$R_{13}$	4.10
	$\theta$	77.13
$\text{Na}_3\text{K}_1$	$R_{\text{KNa}_A}$	3.98
	$R_{\text{KNa}_B}$	3.61
	$R_{\text{KNa}_C}$	3.98
	$R_{\text{Na}_A\text{Na}_B}$	3.47
	$R_{\text{Na}_B\text{Na}_C}$	3.47
	$R_{\text{Na}_A\text{Na}_C}$	6.45
$\text{Na}_2\text{K}_2$	$R_{\text{K}_A\text{Na}_A}$	3.94
	$R_{\text{K}_A\text{Na}_B}$	3.94
	$R_{\text{K}_B\text{Na}_A}$	3.94
	$R_{\text{K}_B\text{Na}_B}$	3.94
	$R_{\text{K}_A\text{K}_B}$	4.10
	$R_{\text{Na}_A\text{Na}_B}$	6.74
$\text{Na}_1\text{K}_3$	$R_{\text{K}_A\text{Na}}$	4.01
	$R_{\text{K}_B\text{Na}}$	3.62
	$R_{\text{K}_C\text{Na}}$	4.01
	$R_{\text{K}_A\text{K}_B}$	4.52
	$R_{\text{K}_B\text{K}_C}$	4.52
	$R_{\text{K}_A\text{K}_C}$	7.64

<sup>a)</sup> Optimized at UCCSD(T) level of theory correlating also the inner-shell electrons as reported in Ref. 34.

**Table 2** Results obtained for the Na<sub>4</sub> cluster for different methods

property*	CCSD(T)			MP2
	All-electron	def2-TZVPP	VTZ	def2-TZVPP
$R_{12}$	3.50	3.61	3.61	3.63
$R_{13}$	3.50	3.61	3.60	3.63
$R_{24}$	3.50	3.61	3.60	3.63
$R_{34}$	3.50	3.61	3.61	3.63
$R_{14}$	3.16	3.25	3.24	3.22
$\angle$	180	180	180	180

\*Distances are given in Å, dihedral angle ( $\angle$ ) in degrees.

ment with the cc-pVTZ on the optimized geometry. Thus, it seems reasonable to expect a similar level of accuracy between the two for the other clusters. Another feature of Table 2 is the evidence that a calculation which does not correlate all the electrons can achieve fairly good outcomes that match the ones yielded by all-electron calculations with an error of around 0.1 Å. Therefore, based on the above discussion, the subsequent calculations presented here employ only frozen core orbitals.

Since coupled cluster calculations become quickly unpractical for larger clusters, further approximated methods must be considered. We used the Na<sub>4</sub> system to exemplify how MP2 calculations compare with the benchmark all-electrons coupled cluster ones. As seen in table 2, the MP2 results are very close to the CCSD(T) ones, and the major source of error seems to be the lack of core correlation, instead of the use of MP2 calculations rather than CCSD. A similar result was obtained for pure small sodium clusters in Ref. 33, and strongly indicates that MP2 calculations can be trusted for the overall shape of the clusters.

For larger clusters there are a vast number of possible compositions, which we try to explore, preferring the symmetric ones whenever possible. The trigonal bipyramid and octahedron shapes, predicted by the Gupta potential for 5 and 6 atoms, respectively, are again in conflict with the available results using all-electron methods in the literature<sup>32,33,37,38</sup> for the pure clusters, which predicted a planar C<sub>2v</sub> structure for the 5 atoms cluster and a pentagonal pyramid for the 6 atoms case. Our CCSD(T) calculations on the Na<sub>5</sub>K<sub>1</sub> mixture corroborates with this shape and found that the lowest energy isomer is the one with the potassium atom lying on the top of the pyramid, although the energy difference is less than 1 kcal mol<sup>-1</sup>. Nevertheless, another important result here is that the MP2 calculations were also sufficient to predict both the correct 5 atoms planar C<sub>2v</sub> and 6 atoms pentagonal pyramid shapes and thus may be employed where CCSD(T) calculations are prohibitive.

The first result where the Gupta potential prediction matched the accurate *ab initio* data available in the literature<sup>32</sup>

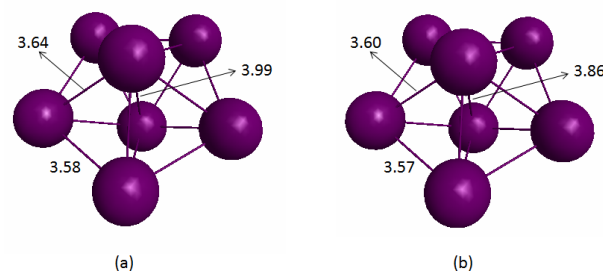


**Fig. 6** Comparison between Na<sub>7</sub> structures provided by (a) Gupta potential and (b) MP2 with 6-311+G\* basis set. Bond lengths are given in Å.

was found for the seven sodium atoms cluster. It corresponds to a pentagonal bipyramid structure and presents D<sub>5h</sub> symmetry. Our MP2/6-311+G\* reoptimization performed for the doublet state agrees with the above results, with a slightly more contracted geometry reached in comparison with the GA, as evidenced in Fig. 6. As shown in Fig. 7, the essentially pentagonal bipyramid shape was maintained for the alloys, but distorted due to different bond lengths among different atoms.

As the GA methodology has shown itself effective in providing initial guesses for this nuclearity, only a few steps were necessary for the reoptimization of all the composomers at the MP2 level. After this reoptimization, in comparison to the Gupta results, a little contraction tendency could, in general, be observed as well, but mainly among the sodium atoms. For the pure potassium 7 atom cluster, the bonds which lie in the plane formed by the pentagon became tighter after the MP2 calculations, while all the others were stretched.

We have also explored quartet states, where true minima could only be found for Na<sub>3</sub>K<sub>4</sub>, Na<sub>4</sub>K<sub>3</sub>, Na<sub>5</sub>K<sub>2</sub> and Na<sub>6</sub>K<sub>1</sub> (at least at MP2 level). The geometries are shown in Fig. 7, while the energy difference between quartet and doublet states ( $\Delta E = E_{\text{quartet}} - E_{\text{doublet}}$ ) are respectively, 68.0, 76.7, 80.3 and 83.5 kJ mol<sup>-1</sup>, suggesting more stable doublet states. Moreover, the geometries predicted by the Gupta potential are closer to the calculations on the doublet states as can be seen in Fig. 7.

For clusters of 8 atoms the Gupta results are again in agreement with the MP2 calculations for mixed clusters studied in this work and the Na<sub>8</sub> from Ref. 33, which is an indicative that the Gupta potential may be used as a reference for larger clusters. Both the Na<sub>7</sub>K<sub>1</sub> and Na<sub>1</sub>K<sub>7</sub> from Figs. 2 and 3 could be optimized with MP2 calculations, and even different isomers were obtained for Na<sub>7</sub>K<sub>1</sub>. For the latter cluster, the most stable isomer was found to be that predicted in the GA approach, which shows the larger K atom on the periphery of the structure, indeed presenting the previously mentioned tendency of potassium atoms not to occupy inner positions in the NaK al-

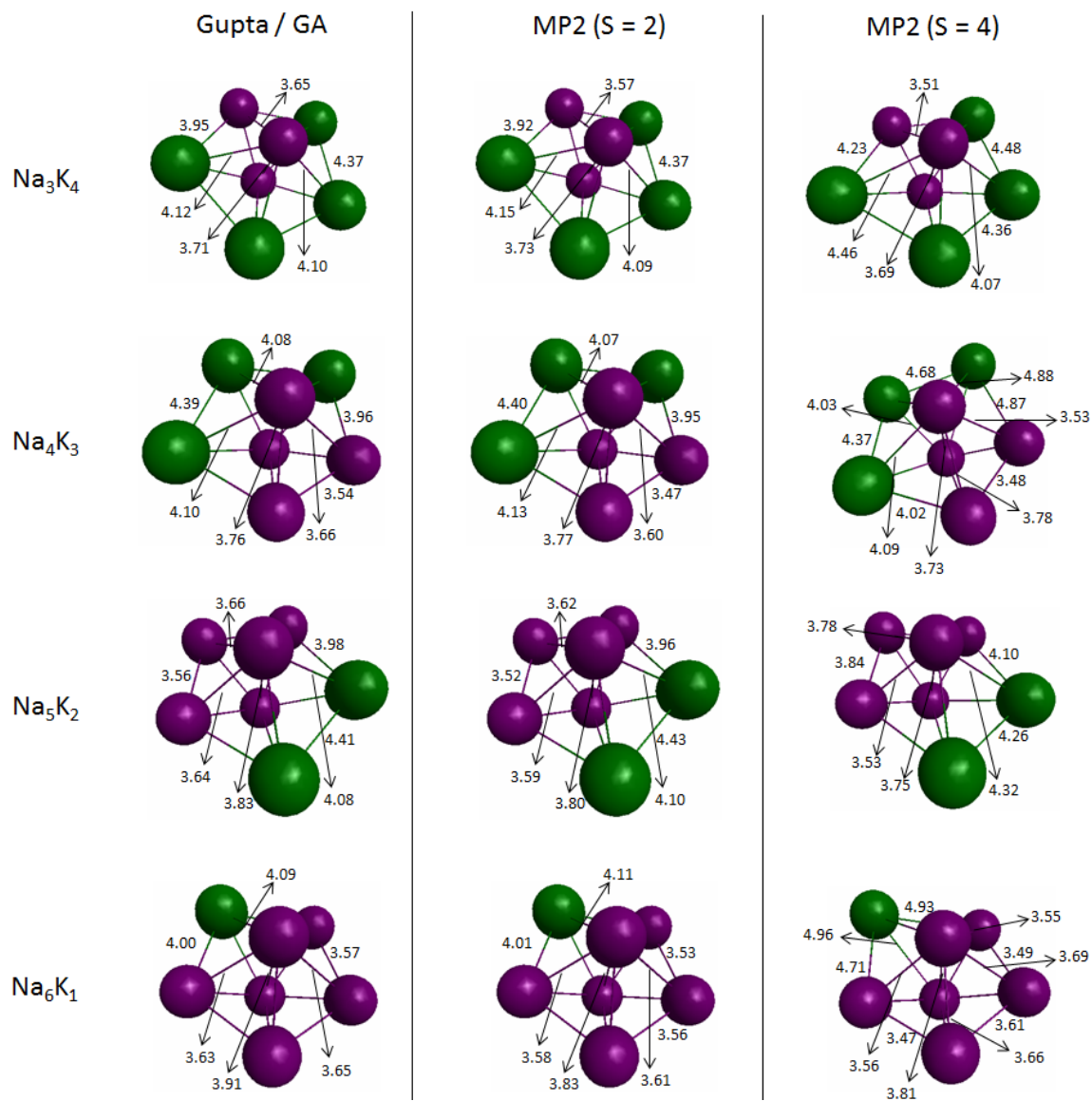


**Fig. 7** Comparison between minima provided by Gupta/GA methodology and by MP2 with 6-311+G\* basis set for doublet and quartet states of 7 atom (Na-K) clusters. Bond lengths are given in Å and the colour pattern follows previous figures.

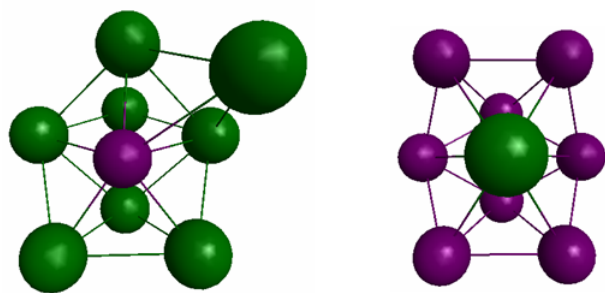


**Fig. 8** Most stable structures yielded by MP2 calculations with LANL2DZ basis set for  $\text{Na}_1\text{K}_8$  (left) and  $\text{Na}_8\text{K}_1$  (right).

loy systems.

We have also employed MP2 with LANL2DZ basis set to explore the doublet state of  $\text{Na}_1\text{K}_8$  and  $\text{Na}_8\text{K}_1$ . At this level of calculation, two different isomers were confirmed as minima for each of the nine atoms alloy studied, and none of them were in agreement with the Gupta results. The most stable isomers are shown in Fig. 8.

For  $\text{Na}_1\text{K}_9$ , again the Gupta/GA structure of Fig. 3 was confirmed by MP2 calculations with a central sodium atom surrounded by potassium, although the  $\text{Na}_9\text{K}_1$  optimized structure showed an imaginary frequency. Therefore, it is hard to state in advance whether the Gupta potential result will be the true structure or not, although the discussion above indicates its lower limits. Since calculations for larger numbers of atoms are very time-consuming, we turn our attention to the choice of a good functional for DFT calculations on these larger systems.

### 3.3 DFT calculations

After analysing trustworthy *ab initio* results for smaller clusters, we can explore different approaches of performing DFT calculations and judge how accurate they perform. Specially if further calculations for larger numbers of atoms are desirable, this analysis would be an important reference point. We therefore compare in table 3 the all-electron correlated coupled cluster results from the previous section (referred here as benchmarks) with DFT results using different functionals and basis sets. As can be seen, DFT calculations not always were capable of obtaining the correct structures, for example, the common B3LYP approach does not predict the  $\text{Na}_1\text{K}_2$  minimum found at the benchmark level. The other qualitative error that can be seen in this table is that the symmetric  $\text{Na}_1\text{K}_3$  structure (at the CCSD(T) level) was obtained as a transition state, which led to a distorted minimum (the one reported in the table). Only the SVWN5 functional employing the LANL2DZ basis provided the correct symmetric structure. Despite of

these errors, fairly good results were obtained for the other systems. The accuracy of the geometries achieved with the def2-TZVPP basis set together with the SVWN5 functional must be highlighted, since it was the only tested approach to correctly predict the benchmark structures within a maximum angle and bond length deviation of 5% and 3%, respectively. All the results shown in table 3 were confirmed as minima by vibrational analysis.

The use of an effective core potential was exploited with the LANL2DZ basis set<sup>39,40</sup>, which treats explicitly the outermost core orbitals along with the valence ones for elements from K to Au through the periodic table<sup>40</sup>. This seems to enable valence electron calculations to be carried out with essentially the same accuracy as all electron calculations but computationally much less demanding<sup>40</sup>. In the following discussion these functionals and basis sets are also compared to the *ab initio* results outside the set of our benchmark results.

A planar  $D_{2h}$  configuration for the pure four atoms clusters was reached for the singlet state within the DFT approach, as experimentally predicted in Ref. 31 for the  $\text{K}_4$  cluster. The LANL2DZ+ECP with PBE, PW91 and SVWN5 functionals, as well as the SVWN5/def2-TZVPP level were tested for both  $\text{Na}_4$  and  $\text{K}_4$ , and some of the results are shown in Fig. 9 together with all-electron correlated CCSD(T) results. The comparison between  $\text{K}_4$  at CCSD(T) level correlating all the electrons and the DFT results shown in Fig. 9 exhibits an even better result when using the effective core potential.

The GA approach wrongly predicts the structures with minimal energy of the four atoms clusters to be tetrahedrons (as mentioned before). Clearly, the empirical potential cannot distinguish different spin multiplicities, and we explored here the triplet state at DFT level, where different minima were obtained, and are shown in Fig. 10. When the tetrahedron provided by the GA was used as a starting point for a DFT re-optimization, the  $\text{K}_4$  cluster was deformed, producing a structure between the initial tetrahedron and the planar one, which corresponds to an oblate tetrahedron, as also analysed and determined in Ref. 41. Analogous results were obtained for the triplet state of the  $\text{Na}_4$ , for which similar prediction is found in Ref. 38. For the quintet state an expanded tetrahedron was obtained for the def2-TZVPP and LANL2DZ (with ECP) basis sets for all functionals tested, for both  $\text{Na}_4$  and  $\text{K}_4$ . The obtained singlet states are, on average, 15.3 and 21.2  $\text{kJ mol}^{-1}$  more stable than the triplet ones for the  $\text{K}_4$  and  $\text{Na}_4$ , respectively. The quintet state of  $\text{K}_4$  lies 103  $\text{kJ mol}^{-1}$  above the singlet one, while the quintet state of  $\text{Na}_4$  is more than 120  $\text{kJ mol}^{-1}$  higher than the ground one. A more specific and detailed study on the triplet and quintet states of  $\text{K}_4$  and  $\text{Na}_4$ , which corroborates the shapes discussed here for these clusters is found in Ref. 41.

For the four atoms alloy case, the structures yielded by DFT for the singlet state resemble the CCSD(T) results in Fig. 5,

**Table 3** Comparison between the benchmark results and several DFT approaches. The results are reported as differences (benchmark minus DFT).

property	benchmark	B3LYP	SVWN5	SVWN5	PBE	
		def2-TZVPP	def2-TZVPP	LANL2DZ+ECP	LANL2DZ+ECP	
Na <sub>2</sub> K <sub>1</sub>	$R_{KNa_A}$	3.70	0.02	0.12	-0.03	-0.08
	$R_{KNa_B}$	3.70	0.02	0.12	-0.03	-0.08
	$\theta$	62.69	-4.19	-2.12	-8.73	-5.23
Na <sub>1</sub> K <sub>2</sub>	$R_{NaK_A}$	3.72	<sup>a)</sup>	0.14	-0.01	-0.07
	$R_{NaK_B}$	3.69	<sup>a)</sup>	0.11	-0.04	-0.10
	$\theta$	100.69	<sup>a)</sup>	-1.85	8.41	1.58
Na <sub>3</sub> K <sub>1</sub>	$R_{KNa_A}$	3.98	-0.01	0.11	-0.06	-0.11
	$R_{KNa_B}$	3.61	0.07	0.16	0.02	-0.03
	$R_{KNa_C}$	3.98	-0.01	0.11	-0.06	-0.11
	$R_{Na_A Na_B}$	3.47	0.01	0.09	-0.25	-0.22
	$R_{Na_B Na_C}$	3.47	0.01	0.09	-0.25	-0.22
	$R_{Na_A Na_C}$	6.45	-0.04	0.14	-0.40	-0.38
Na <sub>2</sub> K <sub>2</sub>	$R_{K_A Na_A}$	3.94	0.00	0.12	-0.08	-0.13
	$R_{K_A Na_B}$	3.94	0.00	0.12	-0.08	-0.13
	$R_{K_B Na_A}$	3.94	0.00	0.12	-0.08	-0.13
	$R_{K_B Na_B}$	3.94	0.00	0.12	-0.08	-0.13
	$R_{K_A K_B}$	4.10	0.09	0.22	0.20	0.06
	$R_{Na_A Na_B}$	6.74	-0.04	0.16	-0.30	-0.32
Na <sub>1</sub> K <sub>3</sub>	$R_{K_A Na}$	4.01	-0.70	-0.26	-0.07	-0.55
	$R_{K_B Na}$	3.62	-0.30	0.08	0.01	-0.11
	$R_{K_C Na}$	4.01	0.40	0.39	-0.07	-0.14
	$R_{K_A K_B}$	4.52	0.48	0.48	0.14	0.28
	$R_{K_B K_C}$	4.52	-1.83	-0.46	0.14	-0.54
	$R_{K_A K_C}$	7.64	-0.65	0.03	0.02	-0.37

<sup>a)</sup> The method did not optimized this minimum.

with essentially the same planar shape but with shorter bond lengths. It should be noted once more that such contraction is expected in the CCSD(T) results if correlation of the core electrons is included. Here also the most symmetric form of Na<sub>2</sub>K<sub>2</sub> was found to be the most stable, just as in the CCSD(T) approach previously pointed out in section 3.2. Again, the approach with SVWN5 functional and def2-TZVPP basis set was the most stable one, always presenting approximately the same error compared to the benchmark results, although it could not predict the correct symmetry of the Na<sub>1</sub>K<sub>3</sub> minimum. The approaches with PBE and SVWN5 functionals with LANL2DZ basis set (ECP) were always compatible among each other, except for the Na<sub>1</sub>K<sub>3</sub> system, where only the latter DFT approach could correctly predict the minimum. The B3LYP functional with the def2-TZVPP basis set, despite presenting the best agreement for some clusters, fails to predict the correct minima for Na<sub>1</sub>K<sub>2</sub>, Na<sub>4</sub>, Na<sub>1</sub>K<sub>3</sub> and K<sub>4</sub> and will not be taken into consideration henceforth.

In a triplet state, a planar structure could be reached for

Na<sub>1</sub>K<sub>3</sub> and Na<sub>3</sub>K<sub>1</sub>, but now with two sodium atoms connected by the minor diagonal of the rhombus of the latter. Two isomers were found for the Na<sub>2</sub>K<sub>2</sub> cluster with structures analogous to those of the triplet states of pure four atoms clusters, the oblate tetrahedron. One of them has adjacent equal atoms while the other presents opposite equal atoms, being the first less symmetric and most stable one. A tetrahedron was always the structure found for the quintet state of all the different compositions tested for the four atoms alloy clusters.

Larger alloys were also studied using DFT in order to compare with the MP2 results from the previous section. Due to the results presented in table 3 and discussed so far, we have employed the def2-TZVPP basis set with SVWN5 functional and LANL2DZ (ECP) basis set with SVWN5 and PBE functionals. These three DFT approaches converged to very similar geometries for all structures discussed here.

For five and six atoms alloys, the DFT calculations provided structures in agreement with the literature on the pure clusters<sup>32,33,37,38</sup> of a planar C<sub>2v</sub> structure and a pentagonal

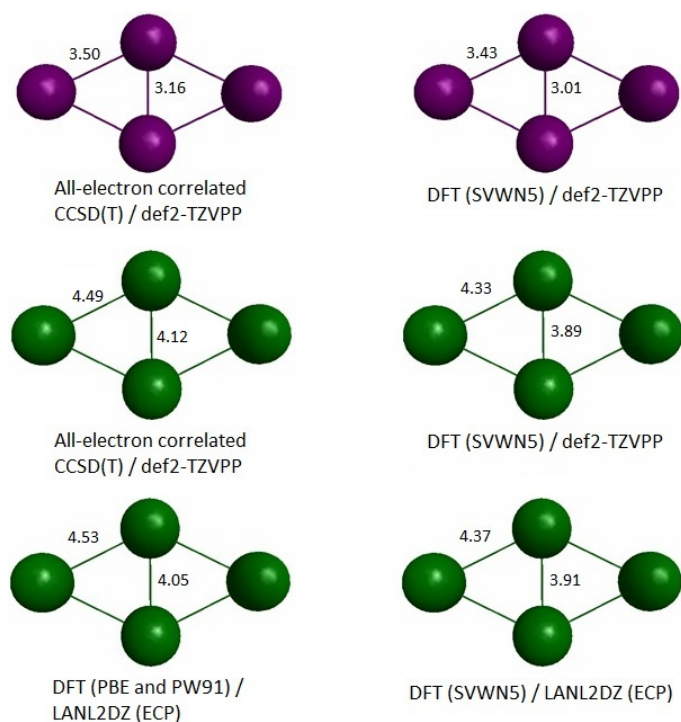


**Fig. 9** Homonuclear four atom sodium clusters (purple) and potassium clusters (green) in a singlet state. All the bond lengths are given in Å.

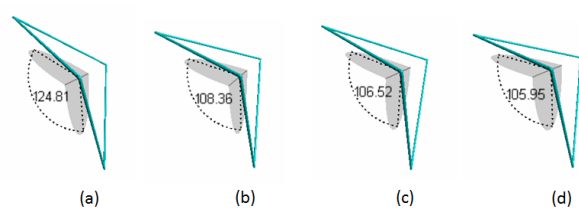


**Fig. 10** Dihedral angle for  $K_4$  triplet state structures yielded by DFT approach at (a) B3LYP level with def2-TZVPP basis set, (b) SVWN5, (c) PW91 and (d) PBE levels, all of those with LANL2DZ basis set with its proper ECP.

pyramid shape, respectively. For the alloy case, the results (shown in Fig. 11 for the 5 atoms case) are in agreement with our MP2 calculations for all composomers tested for these nuclearities and with our coupled cluster calculation for the  $Na_5K_1$ . The pentagonal bipyramid predicted by the Gupta potential and confirmed in a MP2 reoptimization for the seven atoms clusters was also successfully determined by our DFT approach, as well as for clusters of eight atoms such as  $K_8$ ,  $Na_8$ ,  $Na_1K_7$  and  $Na_7K_1$ . The latter structures had their geometries well predicted by the empirical Gupta potential and confirmed as minima in this work through MP2 and DFT calculations, and are also in agreement with Ref. 33. For pure sodium and potassium clusters with nine atoms, the Gupta/GA structures were again confirmed by DFT calculations, which are in agreement with the shape found in Ref. 32. However, a different structure could also be confirmed as minimum for both  $K_9$  and  $Na_9$  clusters within the DFT approach at def2-TZVPP/SVWN5 and LANL2DZ/SVWN5;PBE levels. In particular, the latter  $Na_9$  structure is in agreement with the shape found in Ref. 38 and is more stable than the one found also by the Gupta/GA approach, although the energy difference is less than  $1 \text{ kcal mol}^{-1}$ . For the alloys  $Na_1K_8$  and  $Na_8K_1$ , the Gupta/GA predictions were not confirmed by our DFT approach, which yielded structures that resemble those in Ref. 38 for the pure sodium clusters. In particular, for the  $Na_8K_1$  cluster, one of the DFT structures is in good agreement with our MP2 result. A comparison between these structures is shown in Fig. 12.

For clusters with 10 atoms, however, not even the  $Na_1K_9$  could be confirmed as a minimum within the DFT approach as happened when employing MP2, reinforcing that it is hard to state in advance at which nuclearity the Gupta potential is systematically capable of predicting the true structures.

## 4 Conclusions

We have employed genetic algorithm coupled with an empirical potential to obtain the global minima of  $Na_xK_y$  clusters with  $x + y \leq 15$ . As analyzed, the energy increases (and the average bond energy lowers) as more sodium atoms are substituted by potassium. A general tendency of sodium to occupy the center of the structure and potassium to be segregated at the surface was observed, as expected<sup>1,5</sup>.

Benchmark results employing all-electrons CCSD(T) calculations for the smallest clusters were performed and served as comparison to assess the validity of the Gupta/GA, MP2, and DFT results. Moreover, our CCSD(T) approach on alloys with less than 7 atoms also corroborates with previously reported studies for its pure counterparts in the literature. To the best of our knowledge the structures predicted here for the alloys have not been reported before.

It was also analyzed that the empirical Gupta potential is

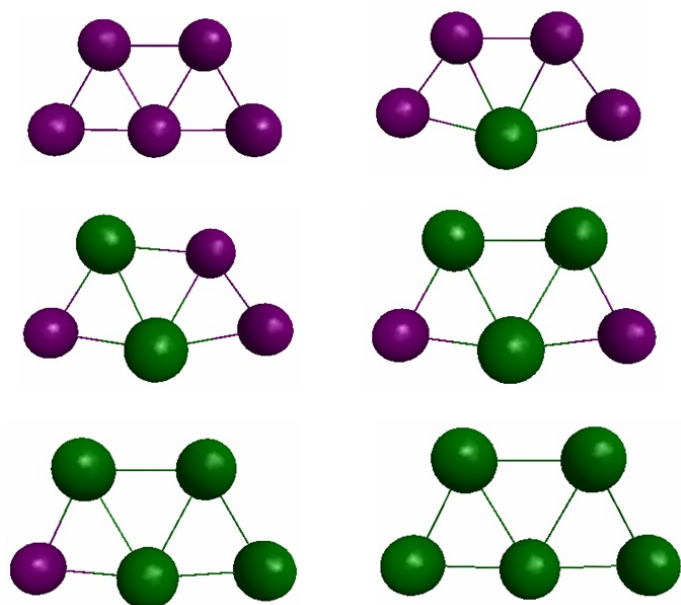


**Fig. 11** Most stable isomers of the 5 atoms clusters yielded by our DFT approach. The colour pattern follows the previous pictures.

improper for clusters with less than seven atoms, but the picture starts to change for this nuclearity, where the pentagonal bipyramid geometry achieved is confirmed by *ab initio* calculations. Even so, errors will occur for larger structures and the results are also not trustworthy after this size.

The MP2 calculations were sufficient to predict correct structures, such as the planar  $C_{2v}$ , pentagonal pyramid and pentagonal bipyramid shapes for the five, six and seven atoms clusters, respectively. Thus, it may be employed where CCSD(T) calculations are prohibitive. Density functional theory calculations were tested for the B3LYP, PW91, PBE and SVWN5 functionals, coupled with def2-TZVPP and LANL2DZ (ECP) basis sets. Despite the good and stable results provided by SVWN5/def2-TZVPP, the SVWN5/LANL2DZ approach is believed to provide the best cost-effective results, yielding deviations of around 5% from the benchmark ones, which may be a well accepted deviation.

## 5 Acknowledgements

BRLG thanks the Conselho Nacional de Desenvolvimento Científico e Tecnológico (CNPq) for the grant 150071/2013-2. The authors also acknowledge the financial support from CNPq, Fundação de Amparo à Pesquisa do estado de Minas Gerais (FAPEMIG) and Coordenação de Aperfeiçoamento de Pessoal de Nível Superior (CAPES).

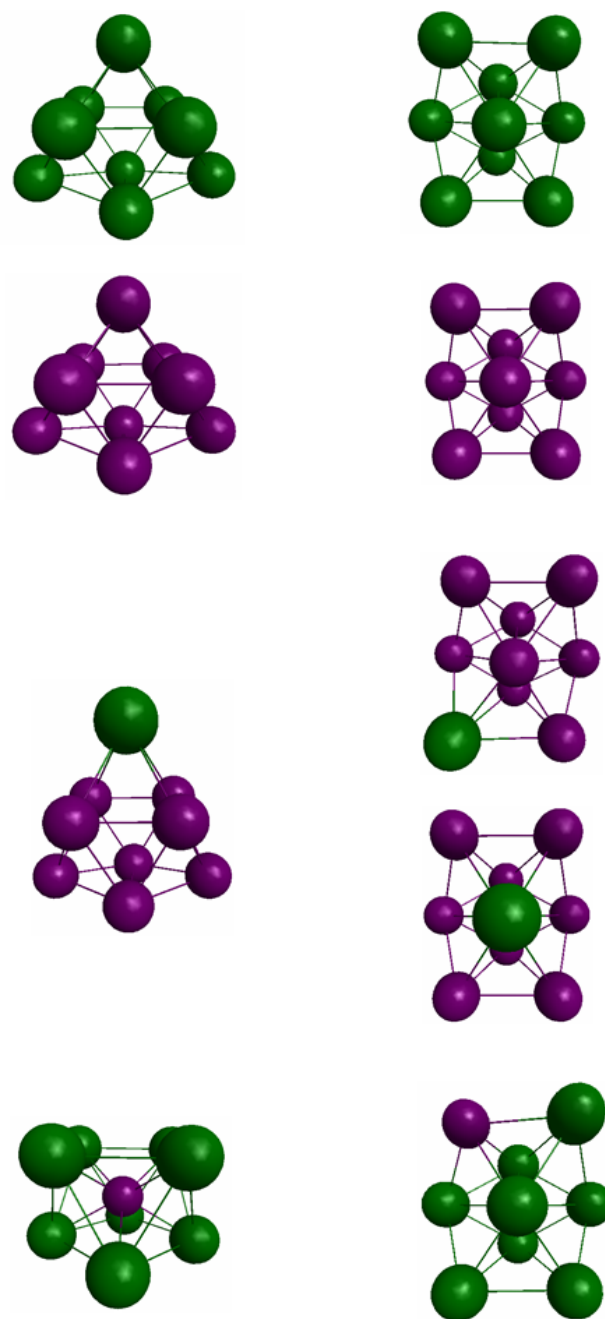


**Fig. 12** Structures of nine atoms yielded by Gupta/GA (left), and minima achieved only by our DFT approach (right). The colour pattern follows the previous pictures.

## References

- 1 M. Tchapyguine, S. Legendre, A. Rosso, I. Bradeanu, G. Öhrwall, S. E. Canton, T. Andersson, N. Mårtensson, S. Svensson and O. Björneholm, *Phys. Rev. B*, 2009, **80**, 033405.
- 2 W.-H. Shih and D. Stroud, *Phys. Rev. B*, 1985, **32**, 804.
- 3 H. Tostmann, E. DiMasi, P. S. Pershan, B. M. Ocko, O. G. Shpyrko and M. Deutsch, *Phys. Rev. B*, 2000, **61**, 7284.
- 4 D. J. González, L. E. González and M. J. Stott, *Phys. Rev. Lett.*, 2005, **94**, 07781.
- 5 A. Aguado and J. M. López, *J. Chem. Phys.*, 2010, **133**, 094302.
- 6 A. Aguado and J. M. López, *J. Chem. Phys.*, 2011, **135**, 134305.
- 7 R. P. Gupta, *Phys. Rev. B*, 1981, **23**, 6265.
- 8 F. Cleri and V. Rosato, *Phys. Rev. B*, 1993, **48**, 22.
- 9 Y. Li, E. Blaisten-Barojas and D. A. Papaconstantopoulos, *Phys. Rev. B*, 1998, **57**, 15549.
- 10 F. F. Guimarães, J. C. Belchior, R. L. Johnston and C. Roberts, *J. Chem. Phys.*, 2002, **116**, 8327.
- 11 Y. Zeiri, *Phys. Rev. E*, 1995, **51**, R2769.
- 12 H. B. Schlegel, *Adv. Chem. Phys.*, 1987, **67**, 249.
- 13 C. Roberts, R. L. Johnston and N. Wilson, *Theoret. Chim. Acta*, 2000, **104**, 123.
- 14 R. A. Lordeiro, F. F. Guimarães, J. C. Belchior and R. L. Johnston, *Int. J. Quantum Chem.*, 2003, **95**, 112–125.
- 15 M. W. Schmidt, K. K. Baldrige, J. A. Boats, S. T. Elbert, M. S. Gorgon, J. H. Jensen, S. Koseki, N. Matsunaga, K. A. Nguyen, S. Su, T. L. Windus, M. Dupuis and J. Montgomery, Jr., *J. Comput. Chem.*, 1993, **14**, 1347.
- 16 T. H. Dunning, *J. Chem. Phys.*, 1989, **90**, 1007–1023.
- 17 R. A. Kendall, T. H. Dunning Jr. and R. J. Harrison, *J. Chem. Phys.*, 1992, **96**, 6796–6806.
- 18 F. Weigend and R. Ahlrichs, *Phys. Chem. Chem. Phys.*, 2005, **7**, 3297.
- 19 K. L. Schuchardt, B. T. Didier, T. Elsethagen, L. Sun, W. Gurumoorthi, J. Chase, J. Li and T. L. Windus, *J. Chem. Inf. Model.*, 2007, **47**, 1045.
- 20 J. D. Watts, J. Gauss and R. J. Bartlett, *J. Chem. Phys.*, 1993, **98**, 8718–8733.
- 21 A. D. Becke, *J. Chem. Phys.*, 1993, **98**, 5648.
- 22 P. J. Stephens, F. J. Devlin, C. F. Chabalowski and M. J. Frisch, *J. Phys. Chem.*, 1994, **98**, 11623.
- 23 R. H. Hertwig and W. Koch, *Chem. Phys. Lett.*, 1997, **268**, 345.
- 24 J. P. Perdew, J. A. Chevary, S. H. Vosko, K. A. Jackson, M. R. Pederson, D. J. Singh and C. Fiolhais, *Phys. Rev. B*, 1992, **46**, 6671.
- 25 J. P. Perdew, K. Burke and M. Ernzerhof, *Phys. Rev. Lett.*, 1996, **77**, 3865.
- 26 J. C. Slater, *Phys. Rev.*, 1951, **81**, 385.
- 27 S. H. Vosko, L. Wilk and M. Nusair, *Can. J. Phys.*, 1980, **58**, 1200.
- 28 M. A. Iron, *Mol. Phys.*, 2003, **101**, 1345–1361.
- 29 S. K. Lai, P. J. Hsu, K. L. Wu, W. K. Liu and M. Iwamatsu, *J. Chem. Phys.*, 2002, **117**, 10715.
- 30 M. K. Harbola, *Proc. Nat. Acad. Sci. USA*, 1992, **89**, 1036–1039.
- 31 A. Kornath, R. Ludwig and A. Zoerner, *Angew. Chem. Int. Ed.*, 1998, **37**, 1575.
- 32 I. A. Solov'yov, A. V. Solov'yov and W. Greiner, *Phys. Rev. A*, 2002, **65**, 053203.
- 33 K. R. S. Chandrakumar, T. K. Ghanty and S. K. Ghosh, *J. Chem. Phys.*, 2004, **120**, 6487.
- 34 A. W. Hauser, C. Callegari, P. Soldán and W. E. Ernst, *J. Chem. Phys.*, 2008, **129**, 044307.
- 35 J. Higgins, C. Callegari, J. Reho, F. Stienkemeier, W. E. Ernst, K. K. Lehmann, M. Gutowski and G. Scoles, *Science*, 1996, **273**, 629–631.
- 36 W. Muller, J. Flesch and W. Meyer, *J. Chem. Phys.*, 1984, **80**, 3297–3310.
- 37 A. Banerjee, T. K. Ghanty and A. Chakrabarti, *J. Phys. Chem. A*, 2008, **112**, 12303–12311.
- 38 V. Bonačić-Koutecký, P. Fantucci and J. Koutecký, *Phys. Rev. B*, 1988, **37**, 4369–4374.
- 39 W. R. Wadt and P. J. Hay, *J. Chem. Phys.*, 1985, **82**, 284–298.
- 40 P. J. Hay and W. R. Wadt, *J. Chem. Phys.*, 1985, **82**, 299–310.
- 41 M. Verdicchio, S. Evangelisti, T. Leininger and A. Monari, *J. Chem. Phys.*, 2012, **136**, 094301.